question. This means that a convergent beam is reflected in the same way as from a bent perfect crystal in Johann or Johansson geometry. Usually, the window is wide enough to transmit an energy band that includes both $K\alpha_1$ and $K\alpha_2$ components of the incident beam. The distributions of these components are projected on the (x, x', λ_1) plane in Fig. 7.4.4.3. The sample is placed in the (para)focus of the beam, and often the divergence of the beam is much larger than the width of the rocking curve of the sample crystal. This means that at any given time the signal comes from a small part of the beam, but the whole beam contributes to the background. The profile of the reflection is a convolution of the actual rocking curve with the divergence and wavelength distributions of the beam. The calculated profile in Fig. 7.4.4.2 demonstrates that in a typical case the profile is determined by the instrument, and the peak-to-background ratio is much worse than with a perfect-crystal monochromator.

An alternative arrangement, which has become quite popular in recent years, is one where the plane of diffraction at the monochromator is perpendicular to that at the sample. The beam is limited by slits only in the latter plane, and the wavelength varies in the perpendicular plane. An example of rocking curves measured by this kind of diffractometer is given in Fig. 7.4.4.4. The $K\alpha_1$ and $K\alpha_2$ components are seen separately plus a long tail due to continuum radiation, and the profile is that of the divergence of the beam.

In the Laue method, a well collimated beam of white radiation is reflected by a stationary crystal. The wavelength band reflected by a perfect crystal is indicated in Fig. 7.4.4.1(*b*). The mosaic blocks select a band of wavelengths from the incident beam and the wavelength deviation is related to the angular deviation by $\Delta\lambda/\lambda = \cot\theta\Delta\theta$. The angular resolution is determined by the divergences of the incident beam and the spatial resolution of the detector. The detector is not energy dispersive, so that the background arises from all scattering that reaches the detector. An estimate of the background level involves integrations over the incident spectrum at a fixed scattering angle, weighted by the cross sections of inelastic scattering and the attenuation factors. This calculation is very complicated, but at any rate the background level is far higher than that in a diffraction measurement with a monochromatic incident beam.

7.4.4.3. *Detecting system*

The detecting system is an integral part of the X-ray optics of a diffraction experiment, and it can be included in the phase-space diagrams. In single-crystal diffraction, the detecting system is usually a rectangular slit followed by a photon counter, and the slit is large enough to accept all the reflected beam. The slit can be stationary during the scan (ω scan) or follow the rotation of the sample ($\omega/2\theta$ scan). The included TDS depends on these choices, but otherwise the amount of background is proportional to the area of the receiving slit. It is obvious from a comparison between Fig. 7.4.4.1 and Fig. 7.4.4.3 that a much smaller receiving slit is sufficient in the parallel-beam geometry than in the conventional divergent-beam geometry. Mathieson (1985) has given a thorough analysis of various monochromator–sample–detector combinations and has suggested the use of a two-dimensional $\omega/2\theta$ scan with a narrow receiving slit. This provides a deconvolution of the reflection profile measured with a divergent beam, but the same result with better intensity and resolution is obtained by the parallel-beam techniques.

The above discussion has concentrated on improving the signal-to-background ratio by optimization of the diffraction geometry. This ratio can be improved substantially by an energy-dispersive detector, but, on the other hand, all detectors have some noise, which increases the background. There have been marked developments in recent years, and traditional technology has been replaced by new constructions. Much of this work has been carried out in synchrotron-radiation laboratories (for

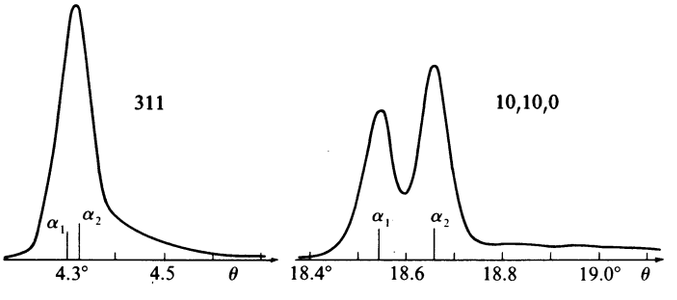

Fig. 7.4.4.4. Two reflections of beryllium acetate measured with Mo $K\alpha$. The graphite (002) monochromator reflects in the vertical plane, while the crystal reflects in the horizontal plane. The equatorial divergence of the beam is 0.8°, FWHM.

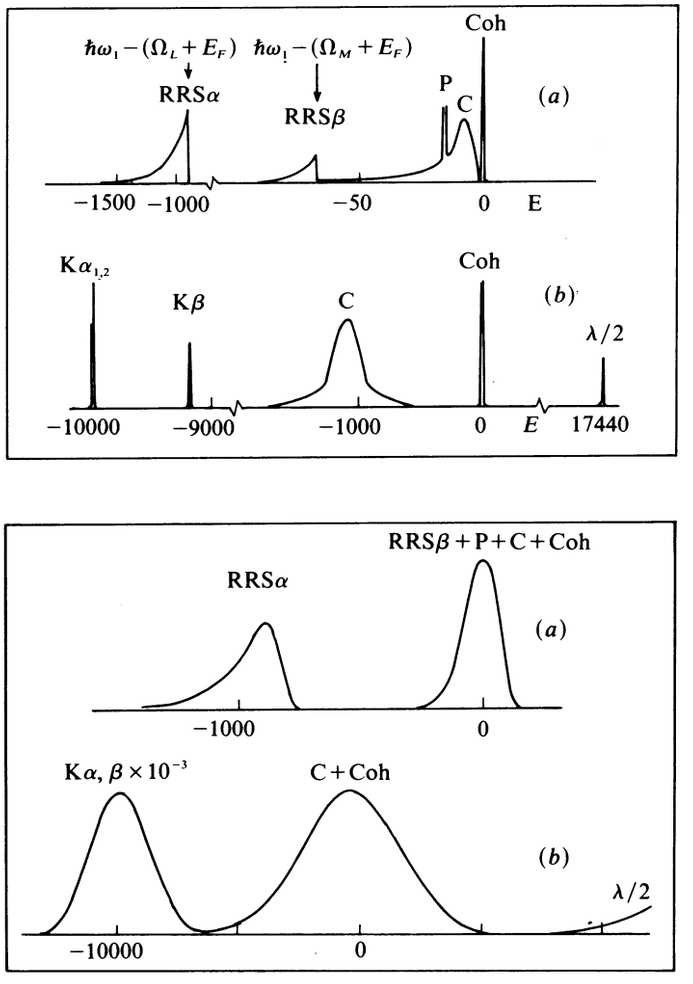

Fig. 7.4.4.5. Components of scattering at small scattering angles when the incident energy is just below the *K* absorption edge of the sample [upper part, (*a*)], and at large scattering angles when the incident energy is about twice the *K*-edge energy [upper part, (*b*)]. The abbreviations indicate resonant Raman scattering (RRS), plasmon (P) and Compton (C) scattering, coherent scattering (Coh) and sample fluorescence ($K\alpha$ and $K\beta$). The lower part shows these components as convoluted by the resolution function of the detector: (*a*) a SSD and (*b*) a scintillation counter (Suortti, 1980).

references, see Thomlinson & Williams, 1984; Brown & Lindau, 1986).

A position-sensitive detector can replace the receiving slit when a reciprocal space is scanned. TV area detectors with an X-ray-to-visible light converter and two-dimensional CCD arrays have moderate resolution and efficiency, but they work in the current mode and do not provide pulse discrimination on the basis of the photon energy. One- and two-dimensional proportional chambers have a spatial resolution of the order of 0.1 mm, and the relative energy resolution, $\Delta E/E \simeq 0.2$, is sufficient for rejection of some of the parasitic scattering.

The NaI(Tl) scintillation counter is used most frequently as the X-ray detector in crystallography. It has 100% efficiency for the commonly used wavelengths, and the energy resolution is comparable to that of a proportional counter. The detector has a long life, and the level of the low-energy noise can be reduced to about 0.1 counts s^{-1}.

The Ge and Si(Li) solid-state detectors (SSD) have an energy resolution $\Delta E/E = 0.01$ to 0.03 for the wavelengths used in crystallography. The relative Compton shift, $\Delta\lambda/\lambda$, is $(0.024\ \text{Å}/\lambda) \times (1 - \cos 2\theta)$, where 2θ is the scattering angle, so that even this component can be eliminated to some extent by a SSD. These detectors have been bulky and expensive, but new constructions that are suitable for X-ray diffraction have become available recently. The effects of the detector resolution are shown schematically in Fig. 7.4.4.5 for a scintillation counter and a SSD.

Crystal monochromators placed in front of the detector eliminate all inelastic scattering but the TDS. The monochromator must be matched with the preceding X-ray optical system, the sample included, and therefore diffracted-beam monochromators are used in powder diffraction only (see Subsection 7.4.4.4).

7.4.4.4. *Powder diffraction*

The signal-to-background ratio is much worse in powder diffraction than in single-crystal diffraction, because the background is proportional to the irradiated volume in both cases, but the powder reflection is distributed over a ring of which only the order of 1% is recorded. The phase-space diagrams of a typical measurement are shown in Fig. 7.4.4.6. The Johansson monochromator is matched to the incident beam to provide

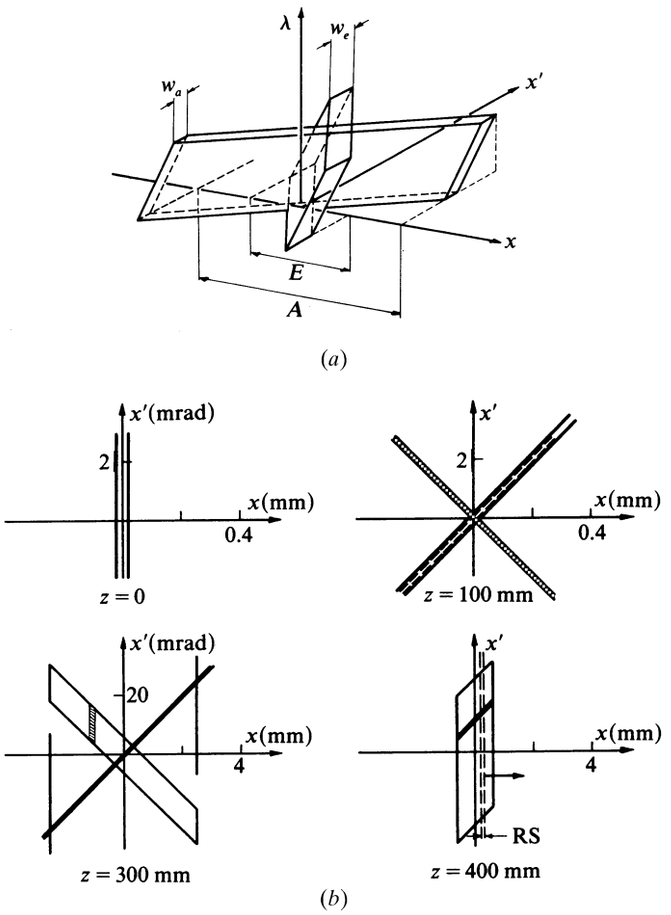

Fig. 7.4.4.6. Equatorial phase-space diagrams for powder diffraction in the Bragg–Brentano geometry. (*a*) The acceptance and emittance windows of a Johannson monochromator; (*b*) the beam in the $\lambda = \lambda_1$ plane: the exit beam from the Johansson monochromator is shown by the hatched area ($z = 100$ mm), the beam on the sample by two closely spaced lines, the reflectivity range of powder particles in a small area of the sample by the hatched area ($z = 300$ mm, note the change of scales), and the scan of the reflected beam by a slit RS by broken lines ($z = 400$ mm, at the parafocus).

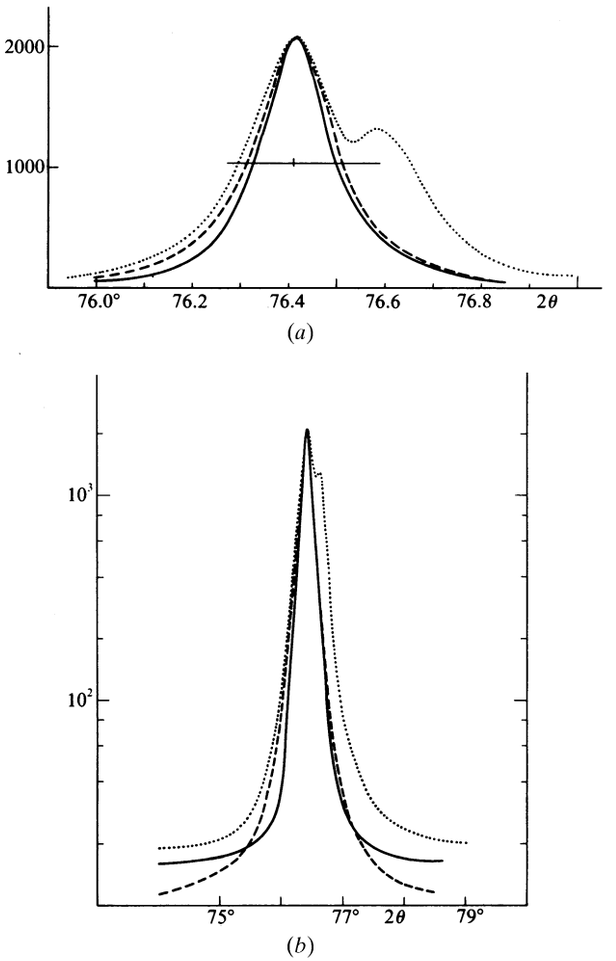

Fig. 7.4.4.7. Three measurements of the 220 reflection of Ni at $\lambda = 1.541$ Å scaled to the same peak value; (*a*) in linear scale, (*b*) in logarithmic scale. Dotted curve: graphite (00.2) Johann monochromator, conventional 0.1 mm wide X-ray source (Suortti & Jennings, 1977); solid curve: quartz (10.1) Johansson monochromator, conventional 0.05 mm wide X-ray source; broken curve: synchrotron radiation monochromatized by a (+, −) pair of Si (111) crystals, where the second crystal is sagittally bent for horizontal focusing (Suortti, Hastings & Cox, 1985). The horizontal line indicates the half-maximum value. In all cases, the effective slit width is much less than the FWHM of the reflection.